The EMBO Journal Vol. 21 No. 7 pp. 1565–1576, 2002

A positive feedback loop stabilizes the guanine-nucleotide exchange factor Cdc24 at sites of polarization

Anne-Christine Butty, Nathalie Perrinjaquet, Audrey Petit[1], Malika Jaquenoud, Jeffrey E.Segall[2], Kay Hofmann[3], Catherine Zwahlen[1] and Matthias Peter[4]

Swiss Institute for Experimental Cancer Research, Chemin des Boveresses 155, CH-1066 Epalinges/VD, [1]Institute of Organic Chemistry, University of Lausanne, CH-1015 Lausanne, Switzerland, [2]Department of Anatomy and Structural Biology, Albert Einstein College of Medicine, 1300 Morris Park Avenue, Bronx, NY 10461, USA and [3]Bioinformatics Group, Memorec Stoffel GmbH, Stöckheimerweg 1, D-50829 Köln, Germany

[4]Corresponding author
e-mail: matthias.peter@isrec.unil.ch

In *Saccharomyces cerevisiae*, activation of Cdc42 by its guanine-nucleotide exchange factor Cdc24 triggers polarization of the actin cytoskeleton at bud emergence and in response to mating pheromones. The adaptor protein Bem1 localizes to sites of polarized growth where it interacts with Cdc42, Cdc24 and the PAK-like kinase Cla4. We have isolated Bem1 mutants (Bem1-m), which are specifically defective for binding to Cdc24. The mutations map within the conserved PB1 domain, which is necessary and sufficient to interact with the octicos peptide repeat (OPR) motif of Cdc24. Although Bem1-m mutant proteins localize normally, *bem1-m* cells are unable to maintain Cdc24 at sites of polarized growth. As a consequence, they are defective for apical bud growth and the formation of mating projections. Localization of Bem1 to the incipient bud site requires activated Cdc42, and conversely, expression of Cdc42–GTP is sufficient to accumulate Bem1 at the plasma membrane. Thus, our results suggest that Bem1 functions in a positive feedback loop: local activation of Cdc24 produces Cdc42–GTP, which recruits Bem1. In turn, Bem1 stabilizes Cdc24 at the site of polarization, leading to apical growth.

Keywords: actin/Bem1/Cdc24/cell polarity/polarized growth

Introduction

The establishment of cell polarity and polarized growth is crucial for the development and functioning of both uni- and multi-cellular organisms (Drubin, 2000). On a cellular level, polarity results in the generation and maintenance of shape, directional movement, phagocytosis, adhesion and motility. All these changes require dynamic assembly and rearrangements of the actin cytoskeleton, which are orchestrated by local activation and inactivation of Rho-type GTPases (Hall, 1998). However, the mechanisms underlying their spatial and temporal regulation remain poorly understood.

The yeast *Saccharomyces cerevisiae* exhibits polarized growth at several stages of its life cycle (Pruyne and Bretscher, 2000). During the cell cycle, activation of the Cdc28-ln kinase triggers polarization of the actin cytoskeleton towards the incipient bud site in the late G_1 phase, while during mating, cells polarize towards their mating partner along a pheromone gradient (Gulli and Peter, 2001). Upon nitrogen starvation, cells elongate from one pole, forming chains of linked cells that spread across the substratum (Kron and Gow, 1995). Central to the initiation of actin polarization is the local activation of the small GTPase Cdc42. Like all members of the Ras superfamily, Cdc42 cycles between an inactive GDP-bound and an active GTP-bound state. GDP/GTP cycling is regulated by the guanine-nucleotide exchange factor (GEF) Cdc24, which promotes GDP dissociation and facilitates GTP binding, whereas the GTPase-activating proteins Rga1 and Bem3 have the opposite effect and stimulate the intrinsic GTPase activity of Cdc42. In the active GTP-bound state, Cdc42 interacts with its downstream effectors, which in turn control the assembly of actin filaments and their organization into complex structures (Johnson, 1999). Cortical actin patches congregate at the site of polarization and actin cables become orientated towards that site, resulting in polarized secretion of vesicles and hence polarized surface growth.

We are interested in the spatial and temporal regulation of Cdc42 during polarized growth. Previous studies suggested that the small GTPase Rsr1/Bud1 targets Cdc24 to the incipient bud site (Bender and Pringle, 1989; Park *et al*., 1997), while, in a pheromone gradient, Far1 delivers Cdc24 to the site of receptor activation marked by Gβγ (Butty *et al*., 1998; Nern and Arkowitz, 1999). Cdc24 is stabilized at the site of polarization, presumably by binding to the adaptor protein Bem1 (Gulli *et al*., 2000). Cells deleted for *BEM1* are viable, but exhibit severe defects in actin organization and polarized growth (Bender and Pringle, 1991; Chenevert *et al*., 1992). After bud emergence, Cdc24 is hyperphosphorylated by Cla4 (Bose *et al*., 2001), and this phosphorylation is thought to trigger its release from Bem1 at the polarization site and thus limit polarized growth (Gulli *et al*., 2000). In addition to Cdc24 (Peterson *et al*., 1994), Bem1 interacts with numerous other proteins including Cdc42 (Butty *et al*., 1998; Bose *et al*., 2001), the PAK-like kinases Ste20 (Leeuw *et al*., 1995) and Cla4 (Gulli *et al*., 2000; Bose *et al*., 2001), Rsr1/Bud1 (Park *et al*., 1997), Boi1 and Boi2 (Bender *et al*., 1996), Far1 (Butty *et al*., 1998) and Ste5 (Lyons *et al*., 1996), and has thus been implicated in many cellular pathways such as signal transduction and morphogenesis. Boi1 and Boi2 interact with the C-terminal SH3 domain of Bem1 (Bender *et al*., 1996),

while Cdc24 binds to its C-terminus (Peterson *et al.*, 1994). However, it is not known whether all binding partners directly associate with Bem1, or whether they bind in a mutually exclusive manner.

To investigate the role of Bem1 during polarized growth, we characterized the molecular interaction between Bem1 and Cdc24 *in vitro* and *in vivo*. We demonstrate that Bem1 and Cdc24 interact directly through two conserved motifs, while the interaction between Far1 and Bem1 is bridged by Cdc24. Importantly, our results suggest that the critical role of Bem1 *in vivo* is to stabilize Cdc24 at sites of polarized growth.

Results

Isolation of BEM1 alleles unable to interact with Far1 and Cdc24

To isolate Bem1 mutants defective for binding to Far1, we designed a two-hybrid screen (see Materials and methods) in which Bem1 was fused to the DNA-binding domain and tagged at is C-terminus with green fluorescent protein (GFP). The GFP fusion did not affect the *in vivo* function of Bem1, and in the two-hybrid assay, Bem1–GFP interacted with Far1 and Cdc42 to the same extent as the non-tagged control (data not shown). A library of randomly mutagenized two-hybrid plasmids was transformed into *EGY48* and screened for loss of interaction with Far1. Promising candidates were re-screened for GFP fluorescence to eliminate mutants that failed to express Bem1 or harbored truncated forms of Bem1. Two Bem1 mutants (referred to as Bem1-m1 and Bem1-m2) were defective for binding to Far1 but interacted efficiently with Cdc42–GTP and thus were used for further analysis.

The interaction between Far1 and Bem1 requires Cdc24

We compared the ability of wild-type Bem1, Bem1-m1 and Bem1-m2 to interact with Far1, Cdc24, Cdc42, Boi1 and Cla4 by two-hybrid analysis (Figure 1; data not shown). In addition, we included the C-terminally truncated Bem1-s1 and Bem1-s2 proteins (Chenevert *et al.*, 1992), as these mutant proteins have been shown previously to be defective for their interaction with Ste20 (Leeuw *et al.*, 1995). All Bem1 mutant proteins interacted efficiently with Cdc42–GTP (Figure 1), confirming that it binds to the N-terminal domain of Bem1 (Bose *et al.*, 2001). Bem1-s1 and Bem1-s2 were both defective for their interaction with Far1, Cdc24 and Cla4, indicating that all these proteins interact with the C-terminal domain of Bem1. As expected, Bem1-m1 was unable to bind to Far1, whereas the interaction of Bem1-m2 with Far1 was strongly reduced (Figure 1). Surprisingly, however, the interaction between Bem1-m1 and Cdc24 was also abolished, and Bem1-m2 binding to Cdc24 was strongly decreased. Co-immunoprecipitation experiments confirmed that Bem1-m1 and Bem1-m2 were defective for binding to Cdc24 (Figure 2A). In contrast to wild-type Bem1 (lane 4), only small amounts of Bem1-m1–GFP (lane 6) or Bem1-m2–GFP (lane 8) co-immunoprecipitated with Cdc24-myc. Finally, the interaction between Bem1 and Cdc24 was also observed in *far1Δ* strains

A Two-hybrid analysis

	Activation domain fusion	DNA binding domain fusion	Miller units +/- SD
EGY48	Far1	Bem1	1769 +/- 74
	Far1	Bem1-m1	2
	Far1	Bem1-m2	101 +/- 1
	Bem1	Far1 (353-830)	636 +/-200
	Bem1-s1	Far1 (353-830)	15 +/-3
	Bem1-s2	Far1 (353-830)	13
	vector	Far1 (353-830)	8 +/-1
	vector	Bem1	6 +/- 1
	Bem1	vector	3
	Cdc24	Bem1	2089 +/- 221
	Cdc24	Bem1-m1	3 +/- 1
	Cdc24	Bem1-m2	941 +/- 79
	Bem1	Cdc24	1465 +/-159
	Bem1-s1	Cdc24	140 +/-3
	Bem1-s2	Cdc24	161 +/- 22
	vector	Cdc24	71 +/- 10
	Bem1	$Cdc42^{C188S}$ GTP bound	1160 +/- 7
	Bem1-s1	$Cdc42^{C188S}$ GTP bound	2200 +/-56
	Bem1-s2	$Cdc42^{C188S}$ GTP bound	1238 +/- 34
	vector	$Cdc42^{C188S}$ GTP bound	303 +/- 11
	$Cdc42^{C188S}$ GTP bound	Bem1	1079 +/- 62
	$Cdc42^{C188S}$ GTP bound	Bem1-m1	1576 +/- 67
	$Cdc42^{C188S}$ GTP bound	Bem1-m2	981 +/- 156
	$Cdc42^{C188S}$ GTP bound	vector	2
957.1far1	Cdc24	Bem1	3177 +/- 39
	vector	Bem1	5 +/- 1
	Cla4	Bem1	113 +/- 7
	Cla4	Bem1-m1	179 +/- 25
	Cla4	Bem1-s2	17 +/- 5
	Cla4	vector	10 +/- 3
	vector	Bem1	2

B

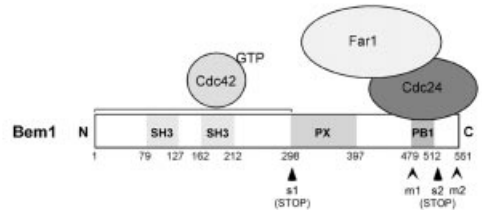

Fig. 1. Two-hybrid analysis of wild-type and mutant Bem1. (**A**) Wild-type and various mutants of Bem1 were tested by two-hybrid analysis in EGY48 cells for their ability to interact with Far1, Cdc24, Cla4 and Cdc42–G12V/C188S ($Cdc42^{C188S}$ GTP-bound). Expression of the β-gal reporter was quantified and is shown as Miller units ± SD. (**B**) Schematic summary of the interactions between Bem1 and Cdc42, Cdc24 and Far1. Cdc42–GTP binds to the N-terminal part of Bem1 and requires an intact second SH3 domain (Bose *et al.*, 2001). The C-terminal PB1 domain interacts with Cdc24. The interaction between Far1 and Bem1 is likely to be bridged by Cdc24.

(Figure 1), demonstrating that Far1 is not required for their binding.

Because both Far1 and Cdc24 were unable to interact with Bem1-m1 and Bem1-m2, they may share the same binding site, or Cdc24 may bridge binding of Far1 to Bem1. To distinguish between these two possibilities, we tested the interaction of Far1 and Bem1 in *cdc24-5* cells, which failed to express detectable amounts of Cdc24 after shifting them to a restrictive temperature for 3 h (Figure 2E). Strikingly, the interaction between Far1 and Bem1 was strongly reduced in *cdc24-5* cells (Table I), suggesting that the interaction between Far1 and Bem1 requires Cdc24 (Figure 1B).

bem1-m cells are unable to phosphorylate Cdc24, although Bem1-m1 and Bem1-m2 interact with Cla4

Phosphorylation of Cdc24 *in vivo* is mediated by Cla4, and requires activated Cdc42 and Bem1 (Gulli *et al.*, 2000; Bose *et al.*, 2001). Unlike wild-type cells, both *bem1-m1* and *bem1-m2* cells failed to phosphorylate Cdc24 (Figure 2C), even after overexpression of Cdc42–GTP

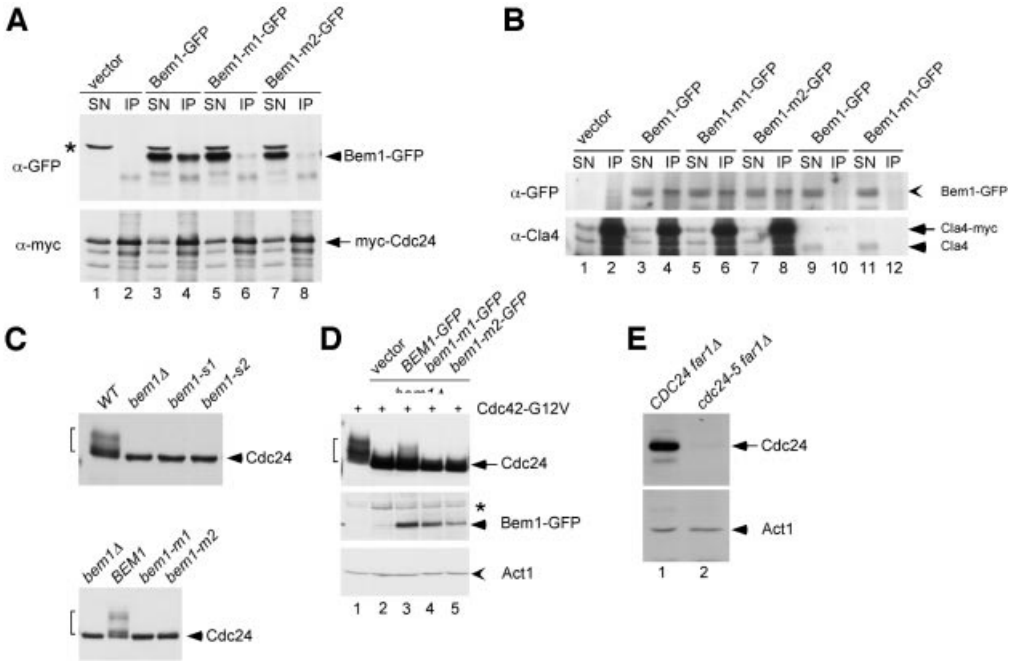

Fig. 2. Interactions between wild-type and mutant Bem1 with Cdc24 and Cla4. (**A**) Cdc24-myc was immunoprecipitated with 9E10 antibodies from cells harboring, as indicated, an empty control vector (lanes 1 and 2) or plasmids allowing expression of wild-type Bem1–GFP (lanes 3 and 4), Bem1-m1–GFP (lanes 5 and 6) or Bem1-m2–GFP (lanes 7 and 8) from the *GAL* promoter. The immunoprecipitates (labeled IP) and cleared cell lysates before immunoprecipitation (labeled SN) were analyzed for the presence of Bem1–GFP (upper panel) and Cdc24-myc (lower panel) by immunoblotting with GFP or 9E10 antibodies, respectively. The asterisk marks an unspecific protein recognized by the GFP antibodies. (**B**) Cla4-myc (lanes 1–8) or extracts from untagged controls (lanes 9–12) were immunoprecipitated with 9E10 antibodies from wild-type cells harboring, as indicated, either an empty control vector (lanes 1 and 2) or a plasmid allowing expression of wild-type Bem1–GFP (lanes 3 and 4), Bem1-m1–GFP (lanes 5 and 6) or Bem1-m2–GFP (lanes 7 and 8) from the *GAL* promoter. The immunoprecipitates and cleared cell lysates were analyzed for the presence of Bem1–GFP (upper panel) and Cla4 (lower panel) by immunoblotting with GFP or Cla4 antibodies, respectively. (**C**) Hyperphosphorylation of Cdc24 was examined in the indicated strains by immunoblotting. The arrowhead points to the position of unphosphorylated Cdc24; the bracket marks the position of hyperphosphorylated Cdc24. (**D**) Wild-type (lane 1) or *bem1Δ* cells (lanes 2–5) were transformed with a plasmid expressing Cdc42–G12V and either an empty control vector (lane 2) or plasmids expressing, as indicated, wild-type or Bem1-m mutant proteins fused to GFP. Hyperphosphorylation of Cdc24 was analyzed by immunoblotting. For control, the extracts were also examined for the presence of Bem1–GFP with GFP antibodies (middle panel) and actin (lower panel). The asterisk marks an unknown protein recognized by the GFP antibody. (**E**) The levels of Cdc24 were compared by immunoblotting of extracts prepared from *far1Δ* (lane 1) and *cdc24-5 far1Δ* cells (lane 2) shifted to 37°C for 3 h. Immunoblotting with antibodies against actin confirmed equal loading (lower panel). Note that *cdc24-5* cells express very low levels of Cdc24, and were thus used as a host for the two-hybrid experiments described in Table I.

Table I. Two-hybrid analysis

Activation domain fusion	DNA-binding domain fusion	Miller units ± SD
cdc24-5 far1Δ		
Far1	Bem1	64 ± 16
Far1	Cdc24	2085 ± 542
Far1	vector	3 ± 1
vector	Bem1	1
vector	Cdc24	6 ± 1
far1Δ		
Far1	Bem1	902 ± 136
Far1	Cdc24	2473 ± 321
Far1	vector	6 ± 2
vector	Bem1	2 ± 2
vector	Cdc24	10

Two-hybrid analysis of wild-type Far1 fused to an activation domain and Bem1 and Cdc24 fused to the LexA-DNA-binding domain performed at 37°C in either *cdc24-5 far1*Δ (YNP39) or *far1*Δ cells (YNP35). Note that *cdc24-5* cells express very low levels of Cdc24, as shown in Figure 2E. Expression of the β-gal reporter was quantified and is shown as Miller units ± SD.

(Figure 2D). Because Cla4 was able to co-immunoprecipitate efficiently with both the wild type and the Bem1-m mutants (Figure 2B), and also interacts with Bem1-m1 by two-hybrid analysis (Figure 1), these results demonstrate that binding of Cdc24 to Bem1 is required for its phosphorylation by Cla4 *in vivo*.

Two conserved protein–protein interaction motifs mediate binding of Bem1 to Cdc24

Sequencing of the *bem1-m1* and *bem1-m2* alleles revealed single non-conservative amino acid substitutions located within the C-terminal domain of Bem1 (Figure 3A), consistent with the previous finding that Cdc24 interacts with the C-terminal domain of Bem1 (Figure 1; Peterson *et al*., 1994; Ito *et al*., 2001). *bem1-m1* harbors an A to C conversion, changing lysine 480 to glutamic acid, while *bem1-m2* contains a C to G mutation that changes serine 547 to a proline residue. Sequence alignment of the C-terminal region of Bem1 from *S.cerevisiae*, its *Schizosaccharomyces pombe* homolog Scd2 (Chang *et al*., 1994) and Bem1 from *Ashbya gossipii* (Figure 3A) revealed a conserved motif, which was recently termed PB1 for phox and Bem1 (Ito *et al*., 2001). The K480E mutation of Bem1-m1 is part of the conserved PB1 core, while the S547P mutation of Bem1-m2 lies further downstream, suggesting that the flanking regions may

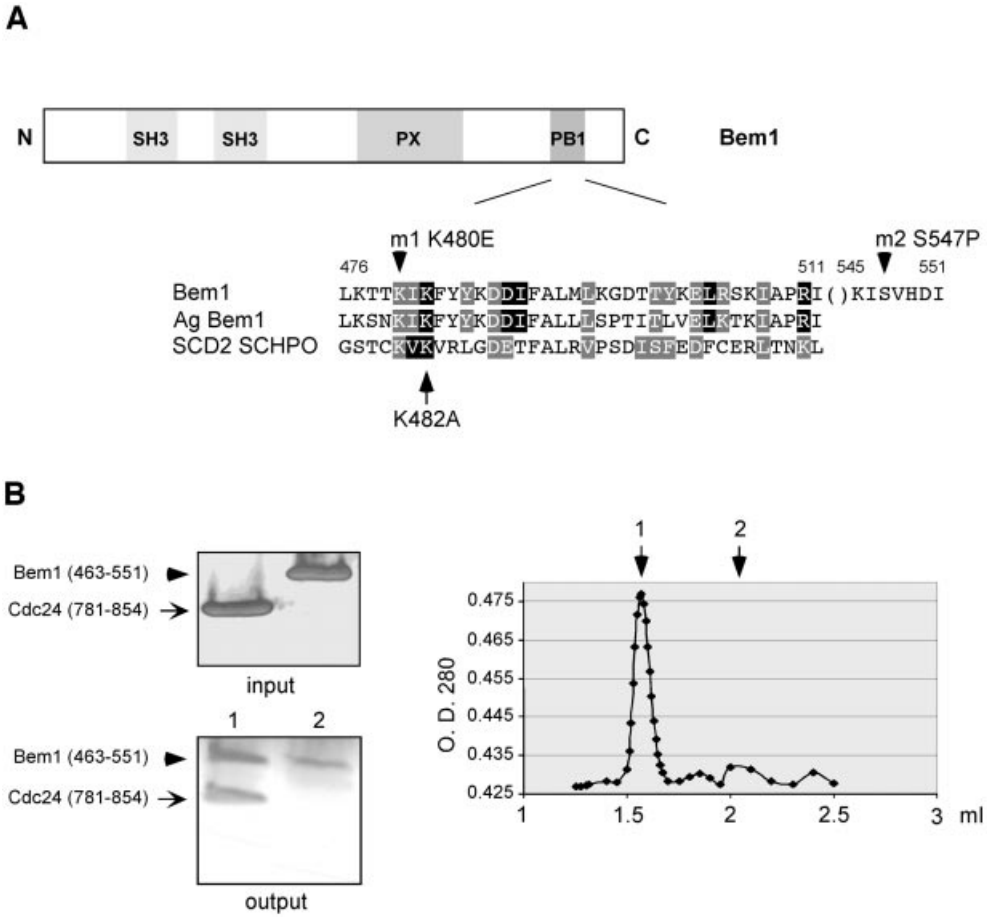

Fig. 3. Identification of a conserved motif in Bem1 sufficient to directly bind to Cdc24. (**A**) Schematic representation of Bem1 with its different domains. PX, PX domain of Bem1; SH3, Src homology domain. The amino acid sequence of a C-terminal motif of Bem1 (termed PB1) from *S.cerevisiae* (Bem1) was aligned with homologs from *A.gossipii* (AgBem1) and *S.pombe* (SCD2). The numbers indicate the amino acids in Bem1 starting from the N-terminal methionine. Identical amino acids are shown with black boxes; similar amino acids are shaded. The mutations found in *bem1-m1* (K480E) and *bem1-m2* (S547P) are indicated by the arrowheads. The mutation determined by Ito *et al*. (2001) is marked by an arrow. (**B**) The PB1 and OPR motifs of Bem1 (amino acids 463–551) and Cdc24 (amino acids 781–854) were expressed in *E.coli* and purified to homogeneity (input). The purified domains were mixed in a 1:1 ratio, separated on a superose 12 gel filtration column, and the fractions examined by spectrometry (right panel). The fractions marked by the arrows were analyzed by SDS–PAGE followed by silver staining (output).

Table II. Two-hybrid analysis in EGY48 cells

Activation domain fusion	DNA-binding domain fusion	Miller units ± SD
Cdc24	Bem1	888 ± 29
Cdc24	Bem1 (463–551)	938 ± 132
Cdc24 (781–854)	Bem1	1220 ± 111
Cdc24 (781–854)	Bem1 (463–551)	1729 ± 85
Cdc24	vector	2 ± 1
Cdc24 (781–854)	vector	2
Vector	Bem1	2
Vector	Bem1 (463–551)	51 ± 13

Two-hybrid analysis of full-length and the indicated fragments of Bem1 and Cdc24. The interaction was quantified as described in the footnote to Table I. Note that the PB1 domain of Bem1 is sufficient to interact with the OPR domain of Cdc24.

contribute to efficient binding to Cdc24. Besides fungal Bem1 proteins, the PB1 motif is found in the N-terminal region of several mammalian signaling proteins including human MEK3, isoforms of protein kinase C and several hypothetical proteins of *Arabidopsis thaliana* (Ito *et al*., 2001).

Two-hybrid assays demonstrated that a small fragment (amino acids 463–551) containing the PB1 domain of Bem1 was sufficient to interact with Cdc24 and Far1 (Table II; data not shown). In contrast, this fragment was unable to interact with Cla4 (data not shown), indicating that this interaction requires determinants outside the PB1 domain. Interestingly, the C-terminus of Cdc24 contains an evolutionarily conserved motif termed octicos peptide repeat (OPR; Ponting, 1996), which is also present in the C-terminus of Scd1, the Cdc24 homolog of *S.pombe*. Constructs encompassing the OPR domain of Cdc24 readily interacted with the PB1 domain of Bem1 by two-hybrid assay (Table II; Ito *et al*., 2001), suggesting that the OPR and PB1 domains may mediate specific binding. Indeed, purified OPR and PB1 domains quantitatively formed heterodimers *in vitro*, as assayed by gel filtration on a superose 12 column (Figure 3B). Thus, the OPR

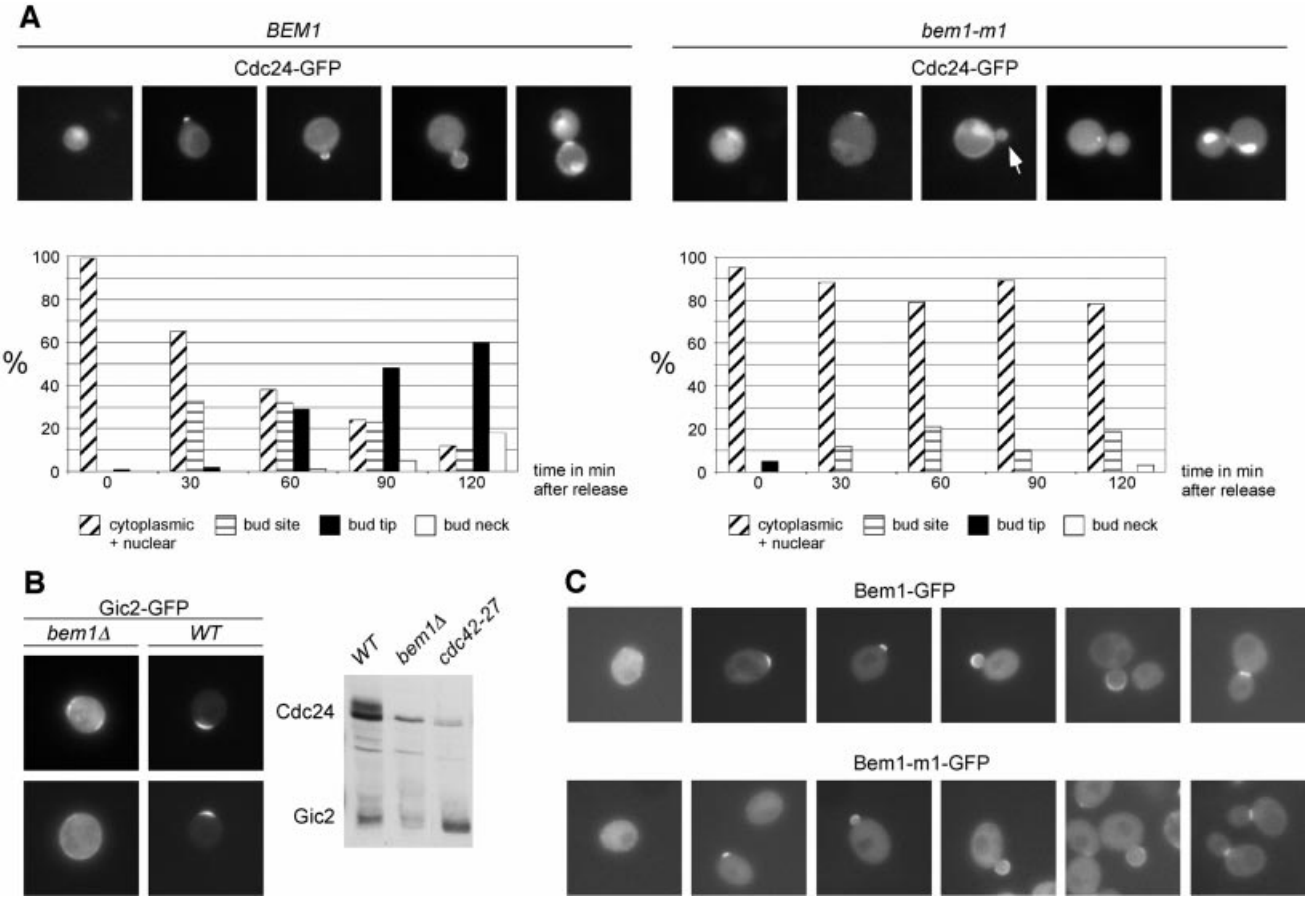

Fig. 4. Binding of Cdc24 to Bem1 is required to maintain Cdc24 at bud tips. (**A**) The localization of Cdc24–GFP expressed from the *ADH* promoter was examined in either wild-type (YNP63; left panel) or *bem1-m1* mutant cells (YNP64; right panel) after synchronization by nutritional starvation. The experiment was quantified (graphs) by counting at least 200 cells every 30 min by fluorescence and phase-contrast microscopy. Note that Cdc24–GFP is recruited to the incipient bud site in *bem1-m1* cells, but it is not found at tips of small buds (arrow). (**B**) The localization of the Cdc42 effector Gic2 (left panel) was examined by GFP microscopy after G_0 release at 37°C in the presence of Lat-A in wild-type (YMP288) or *bem1Δ* (YMP1046) cells. Gic2 and Cdc24 were also analyzed by immunoblotting (right panel). Note that Bem1 is required to concentrate activated Cdc42 at the site of polarization. (**C**) The subcellular localization of Bem1–GFP (YACB302; upper row) and Bem1-m1–GFP (YACB303; lower row) was analyzed by GFP microscopy.

domain of Cdc24 directly interacts with the PB1 domain of Bem1, suggesting that the two motifs comprise novel protein–protein interaction domains.

Cdc24–GFP is recruited to the incipient bud site, but is not maintained at bud tips in bem1-m cells

To determine whether binding of Cdc24 to Bem1 affects the subcellular localization of Cdc24, wild-type and *bem1-m* cells expressing Cdc24–GFP were released from a nutritional block in early G_1, and the localization of Cdc24–GFP was examined by GFP microscopy. In both strains, ~35% of Cdc24–GFP initially localized to the incipient bud site (Figure 4A). However, as in *bem1Δ* cells (Gulli *et al*., 2000), Cdc24 was not detectable at tips of small buds in *bem1-m* cells (arrow), while it was maintained at sites of polarized growth in wild-type cells. The localization of Cla4–GFP was not affected in *bem1-m* cells (data not shown), supporting the observation that the Bem1-m mutant proteins efficiently bind Cla4. Based on the localization and degradation of the Cdc42 effector Gic2 (Figure 4B), *bem1Δ* cells fail to keep activated Cdc42 at the incipient bud site (Figure 4B; Jaquenoud et al., 1998). We conclude from these results that binding of Cdc24 to Bem1 is not required for initial membrane recruitment but to maintain active Cdc24 at the site of polarized bud growth.

To examine the subcellular localization of Bem1 wild type and Bem1-m, we expressed functional GFP fusions from the endogenous *BEM1* promoter in *bem1Δ* cells. Like wild-type Bem1–GFP (Ayscough *et al*., 1997; Gulli *et al*., 2000), Bem1-m1–GFP was distributed throughout the cytoplasm in early G_1 cells and localized to the incipient bud site later in G_1 (Figure 4C). Bem1-m1–GFP was found as a crescent at the tip of small and medium budded cells, and remained all over the cortex in large budded cells, although the staining became progressively weaker. Finally, Bem1–GFP and Bem1-m1–GFP localized to the mother bud neck during mitosis. Therefore, the ability of Bem1 to interact with Cdc24 is not required for its subcellular localization, and the failure of Cdc24–GFP to localize to bud tips in *bem1-m* cells is not caused by a localization defect of Bem1-m1.

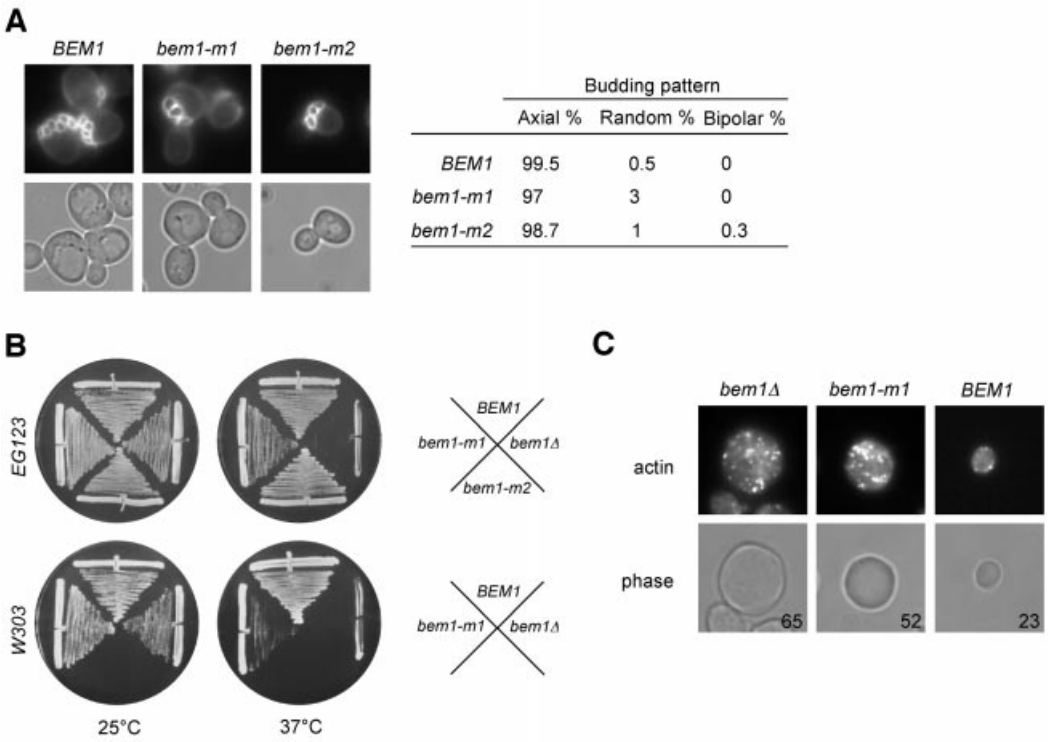

Fig. 5. Budding pattern and growth properties of *bem1-m* mutant cells. (**A**) The budding pattern was quantified in wild-type (YACB302), *bem1-m1* (YACB303) and *bem1-m2* (YACB304) cells in the EG123 background by staining the bud scars with calcofluor white. (**B**) Growth of wild-type, *bem1Δ* and *bem1-m* mutant cells in either the EG123 (upper plates) or W303 (lower plates) background was compared after 2 days on rich medium (YPD) at 25°C (left plates) or 37°C (right plates). (**C**) Wild-type (YMG681), *bem1Δ* (YMP1046) and *bem1-m1* (YMG682) mutant cells (W303 background) were shifted to 37°C for 3 h, and the actin cytoskeleton was examined by fluorescence microscopy after staining with rhodamine–phalloidin. Numbers indicate the percentage (%) of cells with an unpolarized actin cytoskeleton; 300 cells were included in the analysis.

bem1-m cells have a growth defect but exhibit a correct haploid budding pattern

To examine the physiological consequences of cells harboring a Bem1 mutant protein unable to interact with Cdc24, we constructed *bem1Δ* cells expressing wild-type Bem1, Bem1-m1 or Bem1-m2 from the endogenous promoter. Immunoblotting confirmed that all Bem1 proteins were expressed at similar levels (data not shown). We first determined whether *bem1-m* cells exhibit a bud site selection defect when grown at 25°C. As shown in Figure 5A, staining of bud scars by calcofluor white revealed that wild-type as well as *bem1-m* mutant cells in the EG123 background position their buds in the characteristic axial pattern (Chant, 1999), demonstrating that *bem1-m* cells are not defective for bud site selection.

Like *bem1Δ* cells (Chenevert *et al*., 1992), the growth of *bem1-m1* cells was impaired at 37°C, and many cells accumulated with an unpolarized actin cytoskeleton (Figure 5B and C). However, we observed a striking difference of this growth defect depending on the genetic background. For example, while *bem1-m1* in the W303 background was barely viable at 37°C (lower plates), the same mutation in the EG123 background only slightly impaired colony formation (upper plates). The explanation for this difference is not clear at present. We conclude that binding of Cdc24 to Bem1 is not required to interpret the correct positional information during budding, but may be necessary to establish or maintain actin polarization at elevated temperatures.

bem1-m cells are defective for apical bud growth

To examine whether *bem1-m* cells are defective for polarized growth, we first compared the morphology of wild-type and *bem1-m* cells overexpressing the G_1 cyclin Cln2, which is known to trigger an extended phase of apical growth (Lew and Reed, 1993). Strikingly, overexpression of Cln2 in *bem1-m* cells did not cause elongated buds (Figure 6A), although the level of Cln2 was comparable with wild-type strains (right panel). Likewise, cells defective for the E2 ubiquitin-conjugating enzyme Cdc34 exhibited hyperpolarized bud growth, and Cdc24–GFP, Bem1–GFP and Cla4–GFP remain at their tips (Figure 6B; Gulli *et al*., 2000). This phenotype was not reversed by deletion of *SWE1*, suggesting that it is not caused by activation of the morphogenesis checkpoint (Lew and Reed, 1995). Importantly, *cdc34-2 bem1-m* double-mutant cells displayed normal bud morphology (Figure 6B), and Cdc24–GFP was distributed throughout the cytoplasm. In contrast, both Bem1–GFP and Bem1-m1–GFP as well as Cla4–GFP remained at bud tips in the majority of *cdc34-2* and *cdc34-2 bem1-m* mutant cells (Figure 6B), demonstrating that binding of Cdc24 to Bem1 is required to keep Cdc24 at bud tips. Expression of wild-type Bem1 in *cdc34-2 bem1-m1* mutant cells restored polarized growth (data not shown), demonstrating that the Bem1-m1 mutant protein is recessive. These data strongly argue that *bem1-m* cells are defective for apical bud growth because they are unable to maintain Cdc24 at the site of polarization.

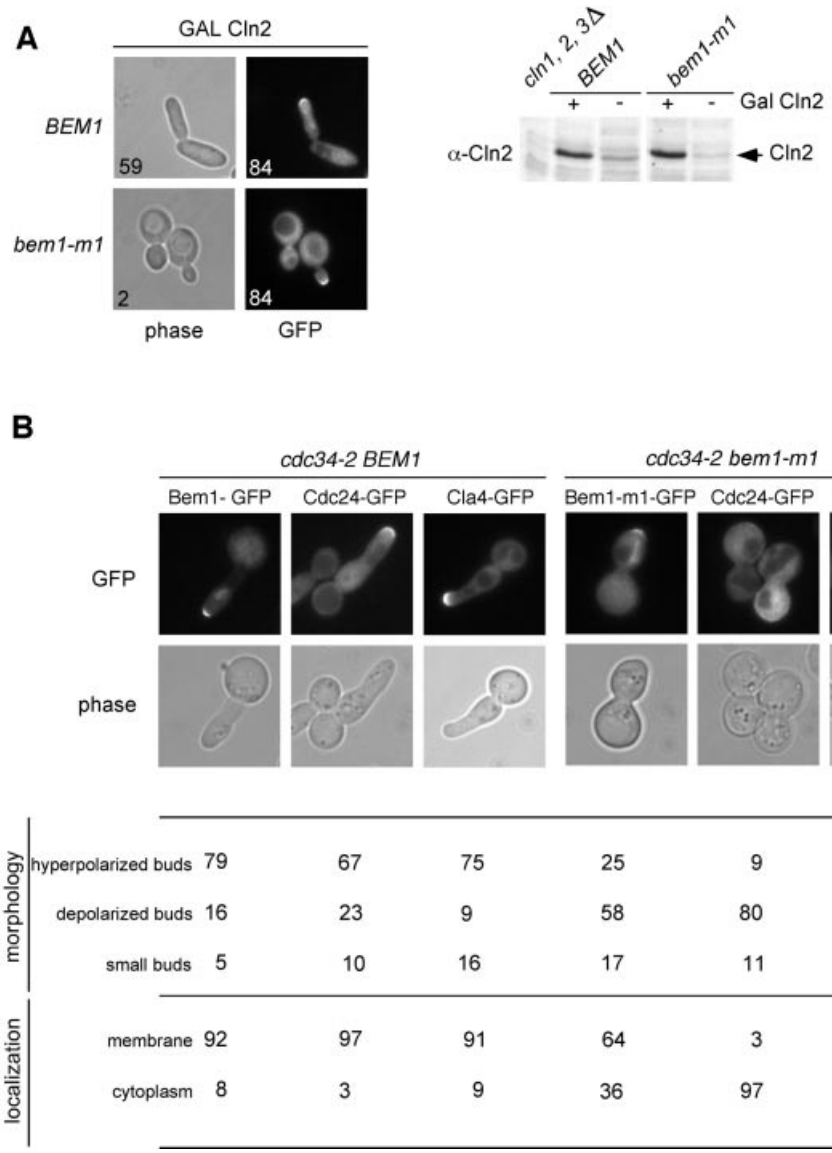

Fig. 6. *bem1-m* cells are defective for apical bud growth. (**A**) Hyperpolarized growth was induced in wild-type (YACB341) or *bem1-m1* (YACB342) cells by overexpression of Cln2 from the *GAL* promoter for 3 h. The localization of Bem1–GFP or Bem1-m1–GFP was visualized by GFP fluorescence (right images). The numbers represent the percentage (%) of hyperpolarized cells (phase) or Bem1–GFP localized at bud tips (GFP). Expression of Cln2 (arrow) was controlled by immunoblotting with Cln2 antibodies (right panel). (**B**) The localization of Bem1–GFP, Bem1-m1–GFP, Cdc24–GFP or Cla4–GFP was analyzed by GFP microscopy (upper rows) in *cdc34-2* or *cdc34-2 bem1-m1* cells after 3 h at 37°C. The phase-contrast images are shown below to visualize the bud morphology. The experiment was quantified as described in (A).

bem1-m cells exhibit a bilateral mating defect, but are able to orientate correctly in a morphogenetic gradient

Because Bem1-m failed to interact with Far1, we tested whether *bem1-m* cells are defective for orientating cell growth towards their mating partner. Indeed, *bem1-m* cells exhibited a bilateral mating defect (Figure 7A), and both *bem1-m1* and *bem1-m2* cells showed a reduced ability to mate with orientation-defective *far1-c* cells (data not shown). *bem1-m* cells were able to efficiently arrest the cell cycle in response to pheromones (Figure 7B), implying that the signal transduction and cell cycle arrest machinery are intact. To directly examine polarization in a morphogenetic gradient, we compared the behavior of wild-type and *bem1-m1* cells in a pheromone gradient using time-lapse microscopy (Segall, 1993). Clearly, >60% of the *bem1-m1* cells were able to polarize towards the position of the highest α-factor concentration compared with 75% of wild-type controls (data not shown), demonstrating that binding of Bem1 to Far1 is not essential for orientating cell polarity in a morphogenetic gradient. Supporting this finding, double-mutant analysis indicated that the mating defects of *bem1-m1* and *far1-c* cells were additive (Figure 7C), implying that they are defective for distinct functions. Consistent with their defect in binding to Cdc24, *bem1-m* mutants have a defect in shmoo formation and actin polarization (Figure 7D), which was partially restored by 10-fold increased pheromone concentrations (Figure 7E). Taken together, these results indicate that *bem1-m* cells exhibit a mating defect, at least in part because they are unable to form mating projections efficiently.

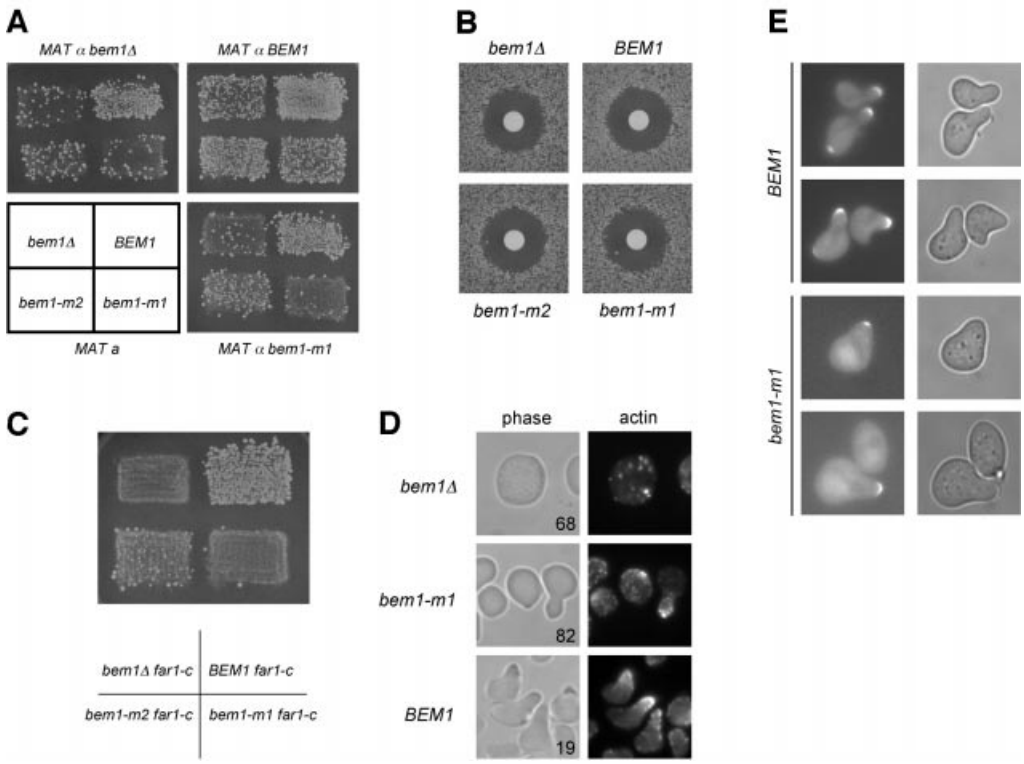

Fig. 7. *bem1-m* cells exhibit a bilateral mating defect and a reduced ability to form polarized mating projections. (**A**) The ability of wild-type (YACB296), *bem1Δ* (YMP459), *bem1-m1* (YACB298) and *bem1-m2* (YACB300) cells to mate with each other was examined by patch mating. Note that *bem1-m* cells exhibit a bilateral mating defect. (**B**) Cell cycle arrest of wild-type (YACB296), *bem1Δ* (YMP459), *bem1-m1* (YACB298) and *bem1-m2* (YACB300) cells in response to pheromones was examined by halo assay. Fifteen micrograms of α-factor were spotted on each filter disc. (**C**) The ability of orientation-defective *far1-c* (YACB288), *bem1Δ far1-c* (YACB36), *bem1-m1 far1-c* (YACB290) and *bem1-m2 far1-c* (YACB292) cells to mate with wild-type cells (IH1793) was analyzed by patch mating. (**D**) The shmoo morphology of wild-type (YMG681), *bem1-m1* (YMG682) and *bem1Δ* (YMP1046) cells (W303 background) was examined by phase-contrast microscopy after addition of 30 nM α-factor for 3 h at 30°C. The actin cytoskeleton was stained with rhodamine–phalloidin and analyzed by fluorescence microscopy. Numbers indicate the percentage of cells with an unpolarized actin cytoskeleton; 300 cells were included in the analysis. (**E**) The polarized localization of Bem1–GFP and Bem1-m1–GFP was analyzed by GFP fluorescence (left panels) and phase-contrast microscopy (right panels) in the indicated strains (EG123 background) treated with 30 nM α-factor for 3 h at 30°C.

Localization of Bem1 to the incipient bud site is dependent on Cdc42–GTP

The localization of Bem1 to the incipient bud site is independent of an intact actin cytoskeleton (Ayscough *et al.*, 1997; Jaquenoud and Peter, 2000), suggesting that Bem1 may interact with a pre-existing component at the cell cortex. Bem1-m or Bem1-s mutant proteins localized to the incipient bud site correctly (Figure 4C; data not shown), indicating that neither binding to Cdc24 nor Cla4 is required for this localization. Interestingly, Bem1–GFP was distributed throughout the cytoplasm in cells arrested in G_1 by the depletion of the G_1 cyclins, but localized to the site of polarized growth when these cells were released by re-expression of Cln2 (Figure 8A). Because Cdc28–Cln is involved in the activation of Cdc42 at bud emergence (Gulli *et al.*, 2000), we examined whether asymmetric localization of Bem1 requires Cdc42–GTP. Wild-type and mutant cells defective for Cdc42 or Cdc24 function were released at 25 or 37°C from a nutritional block in early G_1, and the localization of Bem1–GFP, Cdc24–GFP and the Cdc42 effector Gic2–GFP was examined by GFP microscopy. Interestingly, Bem1 was distributed throughout the cytoplasm in most *cdc42-27* and *cdc24-5* temperature-sensitive cells (Figure 8B), while it was found at the incipient bud site in >80% of wild-type cells (n >200). As expected, the localization of Cdc24–GFP was largely independent of Cdc42 activation, while the localization of the effector Gic2–GFP required both functional Cdc24 and Cdc42 (Figure 8B; Jaquenoud and Peter, 2000). Conversely, Bem1–GFP was recruited to the plasma membrane in G_1-arrested cells overexpressing Cdc42–G12V (Figure 8C), suggesting that Cdc42–GTP is sufficient to localize Bem1. Thus, membrane recruitment or clustering of Bem1 may occur as a result of Cdc42 activation, implying that Bem1 functions at bud emergence after initial activation of Cdc24.

Discussion

Using a mutational approach, we characterized the functional interaction between Cdc24 and Bem1 during cellular polarization. We identified a conserved motif, which is necessary and sufficient to interact with Cdc24, and isolated Bem1 mutant proteins, which specifically failed to interact with Cdc24. *bem1-m* mutant cells are defective for several aspects of polarized growth because

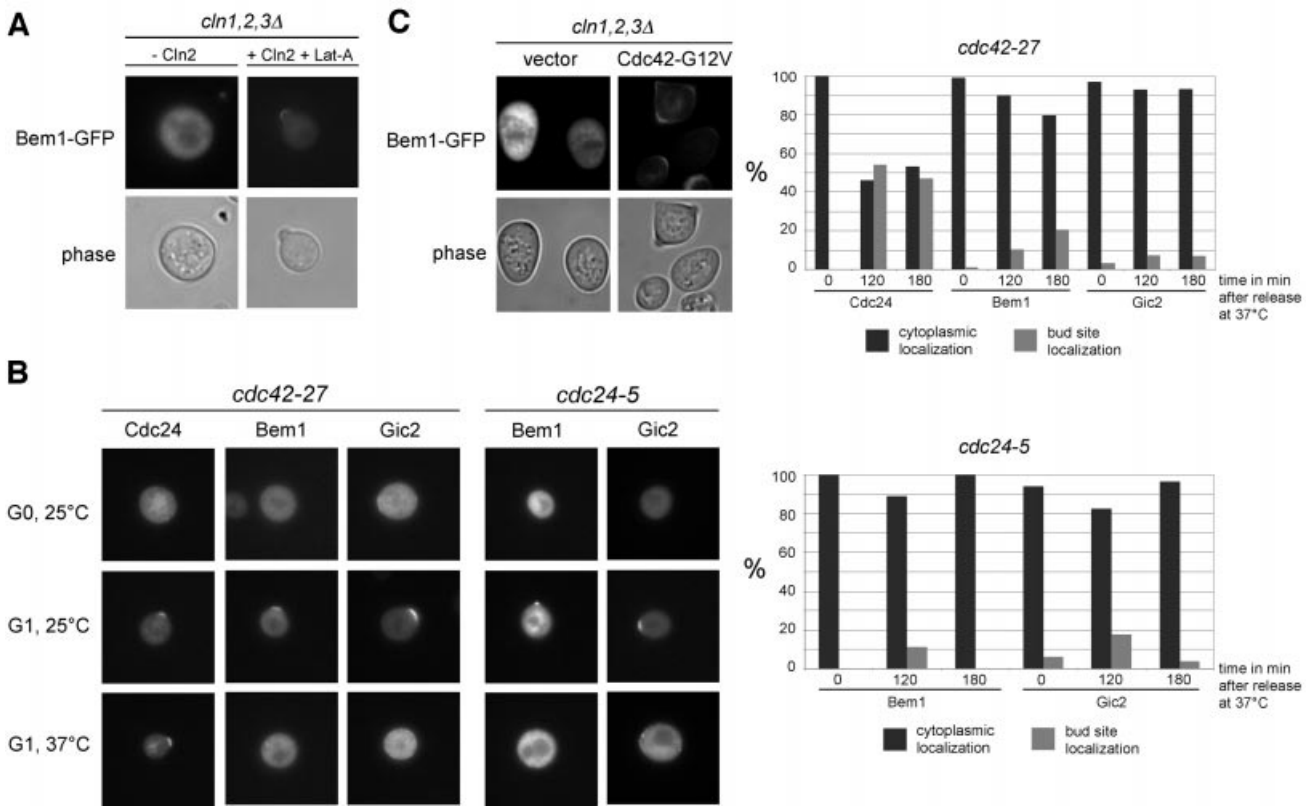

Fig. 8. Recruitment of Bem1 to the incipient bud site requires active Cdc42. (**A**) *cln1, 2, 3Δ pMETCLN2* (YMG258) cells expressing Bem1–GFP from the *ADH* promoter were arrested in G_1 by depletion of Cln2 in medium containing methionine (–Cln2). Cells were quickly washed and Cln2 was induced in medium lacking methionine but containing the actin polymerization inhibitor Lat-A (+Cln2 + Lat-A) to prevent bud emergence. Localization of Bem1–GFP was determined by fluorescence microscopy. (**B**) Temperature-sensitive *cdc42-27* (left panel) and *cdc24-5* (right panel) mutant cells expressing, as indicated, Bem1–GFP, Cdc24–GFP or Gic2–GFP from the *ADH* promoter were released from their block in G_0 either at 25°C or at the restrictive temperature 37°C. The localization of the proteins was examined by GFP fluorescence after the times indicated and quantified by counting at least 200 cells for each time point. (**C**) *cln1, 2, 3Δ pMETCLN2* (YMG258) cells expressing Bem1–GFP from the *ADH* promoter were grown at 30°C in 2% raffinose medium and arrested by depletion of Cln2 as described in (A). Expression of Cdc42–G12V from the *GAL* promoter was induced by addition of 2% galactose for 3 h at 30°C, and the localization of Bem1–GFP was analyzed by fluorescence microscopy.

they are unable to stabilize Cdc24 at the site of growth. Importantly, Bem1 is recruited to the incipient bud site in a Cdc42-dependent manner, implying that Bem1 may be part of a positive feedback loop at bud emergence.

The PB1 motif: a conserved protein–protein interaction domain

Bem1 interacts with Cdc24 through a C-terminal motif termed PB1 (Ito *et al*., 2001), which is both necessary and sufficient to mediate specific binding. The structure of the PB1 motif has recently been solved by NMR spectroscopy, and revealed that the domain shares close similarity with the Ras-binding domain of Raf (Terasawa *et al*., 2001). Interestingly, the PB1 domain interacts with the OPR motif in Cdc24 (Ponting, 1996), and it appears that the PB1 and OPR motifs comprise a conserved protein–protein interaction pair (Ito *et al*., 2001). Cdc24 and its *S.pombe* homolog Scd1 contain adjacent OPR and PB1 motifs in their C-terminus (K.Hofmann, M.Pagni and C.Zwahlen, unpublished results). We therefore speculate that the C-terminus of inactive Cdc24 is inaccessible for Bem1, but that activation of Cdc24 may induce a conformational change allowing binding of Bem1.

Binding of Bem1 to Far1 is bridged by Cdc24

Bem1 interacts with a large number of proteins, but the functional significance of these interactions is not known. Our experiments together with results published previously (Peterson *et al*., 1994; Bose *et al*., 2001) demonstrate that Cdc24 and Bem1 interact directly. However, this is not necessarily the case for all interacting proteins, and it remains to be determined whether these proteins interact simultaneously or in a mutually exclusive manner. Cla4 and Cdc24 both bind to the C-terminal part of Bem1, while Boi1 and Cdc42 require an intact SH3 domain (Bender *et al*., 1996; Bose *et al*., 2001). We were able to separate the binding sites for Cla4 and Cdc24, suggesting that the two proteins can bind simultaneously. Indeed, at least a fraction of Cla4 immunoprecipitates in a trimeric complex with Cdc24 and Bem1 (Gulli *et al*., 2000). Our mutant analysis demonstrates that binding of Cdc24 to Bem1 is required for its phosphorylation by Cla4, implying that Cdc24 is phosphorylated at bud tips when bound to Bem1.

We observed previously that Bem1 interacts with Far1 (Butty *et al*., 1998), an adaptor that links Cdc24 to the activated receptor during mating (Arkowitz, 1999). Although we can not exclude the possibility that Bem1 and Cdc24 interact synergistically with different parts of

Far1, several lines of evidence now suggest that the interaction between Bem1 and Far1 is bridged by Cdc24 (Figure 1B). First, Cdc24 and Bem1 both interact with the C-terminal domain of Far1 (Butty *et al*., 1998). Secondly, Bem1 mutant proteins unable to bind to Cdc24 are also defective for their interaction with Far1. Finally, Bem1 and Far1 fail to bind in cells depleted for Cdc24, while Cdc24 and Far1 interact efficiently in *bem1Δ* cells (Butty *et al*., 1998).

Bem1 maintains Cdc24 at sites of polarized growth, but is dispensable for correct site selection

bem1-m cells exhibit no bud site-selection defect and are able to orientate correctly in a pheromone gradient. Indeed, Cdc24–GFP is correctly recruited to the incipient bud site in synchronized *bem1-m* cells, but disappears from the site of polarization concomitantly with bud emergence. The Bem1-m proteins localize efficiently to the bud site and are maintained at tips of growing buds, suggesting that binding of Bem1 and Cdc24 is not necessary for the correct localization of Bem1. We conclude that site-specific recruitment and initial activation of Cdc24 are independent of Bem1, while maintenance of Cdc24 at sites of polarized growth requires its ability to interact with Bem1.

Binding of Cdc24 to Bem1 is required for apical growth

What are the physiological consequences for cells that fail to stabilize Cdc24 at sites of polarized growth? While these cells are able to polarize their cytoskeleton at bud emergence and are thus viable, they are unable to stabilize the axis of polarization and sustain apical growth. They are defective for apical bud growth, exhibit a reduced ability to elongate during pseudohyphal growth (data not shown), and are unable to efficiently form mating projections. Clearly, *bem1-m* cells exhibit no signaling defect in response to pheromones, suggesting that the interaction between Cdc24 and Bem1 specifically affects polarized growth. Our results suggest that binding of Cdc24 to Bem1 is required to stabilize the axis of polarization determined by activated Gβγ. We speculate that stabilizing Cdc24 at sites of polarized growth is necessary for the continuous local production of Cdc42–GTP.

Bem1 and, in particular, its PB1 domain have been conserved in many fungi, including *S.pombe* and *A.gossipii*. The Bem1 homolog Scd1 in *S.pombe* is essential for polar tip growth (Chang *et al*., 1994), perhaps by maintaining the GEF Scd2 at growing ends. Many aspects of fungal filament formation resemble polarized growth of *S.cerevisiae* (Lengeler *et al*., 2000). By analogy, therefore, we propose that maintaining active Cdc24 at tips of growing filaments may be essential for filament formation and tissue invasion of pathogenic fungi.

A positive feedback loop stabilizes activated Cdc24 at the site of polarized growth

Several lines of evidence suggest that recruitment of Bem1 to the incipient bud site is dependent on activated Cdc42. First, Bem1 directly interacts with Cdc42–GTP (Butty *et al*., 1998; Bose *et al*., 2001). Secondly, membrane localization of Bem1 requires the G_1 cyclins, which are involved in the activation of Cdc42 at bud emergence (Gulli *et al*., 2000). Thirdly, Bem1 is unable to localize to the incipient bud site in *cdc42-27* and *cdc24-5* mutant cells, but its recruitment is independent of other binding partners such as Cla4 (Gulli *et al*., 2000). Finally, expression of mutational activated Cdc42 (Cdc42–G12V) was sufficient to recruit Bem1, but not Cdc24, to the plasma membrane. Taken together, these data support the existence of a positive feedback loop: activation of Cdc24 at the incipient bud site or activated Gβγ in response to pheromones leads to local production of Cdc42–GTP, which in turn recruits Bem1. Bem1 interacts with activated Cdc24 and stabilizes the protein at the cell cortex, thus ensuring continuous production of Cdc42–GTP and apical growth. After bud emergence, Cla4 interacts with Bem1, leading to hyperphosphorylation of Cdc24 at bud tips, and possibly release of Cdc24 from Bem1 (Gulli and Peter, 2001). Thus, both positive and negative feedback loops orchestrate the transient localization of Cdc24 at bud tips.

Materials and methods

Computer searches

Generalized profiles (Bucher *et al*., 1996) were used for database searches and profile-guided multiple alignments, using the PFTOOLS V2.1 package (available from ftp.isrec.isb-sib.ch) as described previously (Weimbs *et al*., 1997). The starting alignment was constructed from the C-terminal regions of Bem1 and its fungal orthologs. During iterative profile refinement, only sequences with error probabilities $p < 0.01$ were included in the next iteration cycle.

Media, yeast strains and genetic manipulations

The yeast strains are described in Table III (see Supplementary data available at *The EMBO Journal* Online). The genotypes of yeast strains used were W303: *ade2-1*, *trp1-1*, *can1-100*, *leu2-3*, *112*, *his3-11*, *15*, *ura3*, *ssd1-d2*; EG123: *trp1-Δ99*, *leu2-Δ1*, *his4-519*, *ura3-52*, *ade2-101*; and Σ1278b: *ura3-52*, unless noted otherwise. Standard yeast growth conditions and genetic manipulations were used as described previously (Guthrie and Fink, 1991). SLAD medium was prepared essentially as described previously (Gimeno *et al*., 1992; Kron *et al*., 1994), except that we used 2% raffinose instead of glucose.

DNA manipulations and two-hybrid assays

Plasmids are described in Table IV (see Supplementary data). Standard procedures were used for recombinant DNA manipulations (Ausubel *et al*., 1991). Oligonucleotides were synthesized by Genset (Paris, France) and are listed in Table V (see Supplementary data). Details of plasmid constructions are available upon request. Two-hybrid assays were performed as described (Brown *et al*., 1997) in *EGY48* or W303-based yeast strains containing the *LacZ* reporter plasmid pSH18.34 (Gyuris *et al*., 1993). Miller units are the average of at least three independent experiments with the standard deviation (SD; SDs below one were omitted).

Isolation of Bem1 mutants unable to interact with Far1

Random mutations were introduced in the pEG202(BEM1–GFP) construct by propagating the plasmid in the *Escherichia coli* strain XL1-Red deficient for DNA repair functions (Stratagene). A library of mutagenized two-hybrid plasmids was transformed into *EGY48* containing the plasmid ACB412 and the *LacZ* reporter gene under the control of the LexA DNA-binding site. Approximately 22 000 transformants were screened for the expression of β-galactosidase (β-gal); ~8.5% of the colonies were white and 1% light blue on X-gal medium. The colonies were re-screened for GFP fluorescence to eliminate mutants that failed to express Bem1 or where Bem1 had been truncated. Plasmids were recovered and retransformed into *EGY48* cells containing the *LacZ* reporter plasmid and either Far1 (ACB412) or Cdc42 (pTP456). Two Bem1 mutants, which failed to interact with Far1 efficiently, interacted with Cdc42–GTP; the *BEM1* coding sequence of these clones (referred to

as *bem1-m1* and *bem1-m2*) was subcloned into pEG203, and these plasmids were used for further analysis.

Antibodies and western blots

Standard procedures were used for yeast cell extracts and immunoblotting (Harlow and Lane, 1988). Polyclonal anti-Cdc24, anti-Bem1, anti-Cla4 and anti-GFP antibodies have been described previously (Leeuw *et al*., 1995; Butty *et al*., 1998; Tjandra *et al*., 1998). 9E10 and monoclonal anti-GFP antibodies were obtained from the ISREC antibody facility. HA11 and anti-actin antibodies were purchased from Babco (Berkeley) and Boehringer Mannheim, respectively, and antibodies against Cln2 from Santa Cruz Biochemicals.

Co-immunoprecipitation experiments

YACB186 cells (*CDC24-MYC*) expressing Bem1–GFP, Bem1-m1–GFP and Bem1-m2–GFP, respectively, from the inducible *GAL* promoter were grown to early log phase in selective media containing 2% raffinose, at which time 2% galactose was added for 2 h. Cells were harvested by centrifugation, resuspended in phosphate-buffered saline (PBS; 137 mM NaCl, 2.7 mM KCl, 4.3 mM Na_2HPO_4, 1.4 mM KH_2PO_4 pH 7.3) containing 20 mM β-glycerophosphate, 50 mM NaF, 1 mM Na_3VO_4 and 1× protease inhibitor cocktail (Roche), and lysed with the One Shot cell extractor (Constant Systems, Warwick, UK) set to maximum pressure (2.8 kbar). The extract was cleared at 10 000 *g* for 5 min, and incubated for 2 h at 4°C with 30 µl of protein G–Sepharose beads (Pharmacia) coupled with 9E10 antibodies. The beads were washed five times with lysis buffer before bound proteins were eluted with gel sample buffer. The eluted proteins were analyzed by immunoblotting with appropriate antibodies. YMP290 cells expressing HA-Bem1–GFP, HA-Bem1-m1–GFP or HA-Bem1-m2–GFP from the constitutive *ADH* promoter were grown in selective media and lysed as described above. The supernatant was incubated for 2 h at 4°C with 30 µl of protein G–Sepharose beads (Pharmacia) coupled with HA11 monoclonal antibodies (Babco). The beads were washed as described, bound proteins eluted with gel sample buffer, and immunoblotted with HA11 or anti-Cdc24 antibodies. Co-immunoprecipitation with myc-Cla4 was essentially carried out as described previously (Gulli *et al*., 2000) using YMG444 and YMG445 cells transformed with plasmids ACB437, ACB479 and ACB482.

Purification of the PB1 and OPR domains, and gel filtration experiments

Escherichia coli cells (BL21) expressing either glutathione *S*-transferase (GST)–Cdc24 (781–854) or GST–Bem1 (463–551) were grown at 37°C to an OD_{600} of 0.7 in Luria–Bertani medium containing 100 µg/ml ampicillin, at which time protein expression was induced by adding 1 mM isopropyl-β-D-thiogalactopyranoside. After 3 h, bacteria were harvested at 4°C by centrifugation at 10 000 *g* for 15 min and resuspended in lysis buffer (150 mM NaCl, 50 mM Tris–HCl pH 7.5, 1 µM EGTA) containing 1× protease inhibitor cocktail (Roche). Cells were lysed by sonication (three cycles of 20 s each) and debris pelleted by centrifugation at 10 000 *g*. The supernatant was incubated for 2 h at 4°C with glutathione–agarose beads (Pharmacia), and washed once with the lysis buffer and twice with thrombin buffer (20 mM Tris–HCl pH 7.5, 100 mM NaCl, 0.5 mM $CaCl_2$). GST was cleaved at 37°C using 10 U of human thrombin (Sigma). Cdc24 (781–854) was further purified on a MonoQ column, and Bem1 (463–551) on a MonoS column, using a SMART system (Amersham Pharmacia Biotechnology GHBH). Proteins were eluted with an increasing NaCl gradient (0.1–1 M), and aliquots were analyzed and quantified by silver staining after separation on a tricine gel. Purified Cdc24 (781–854) and Bem1 (463–551) were mixed in a ratio of 1:1 and incubated at 4°C for 1 h in PBS buffer. The mixture was loaded on a superose 12 PC 3.2/30 column, and aliquots were collected and analyzed by silver staining.

Microscopy, mating assays and budding pattern analysis

Pheromone response and mating assays were performed as described previously (Valtz and Peter, 1997). For shmoo assays, α-factor (Lipal Biochemicals, Zurich) was added for 3 h at 30°C at 50 µg/ml final concentration. Orientation assays with wild-type (YACB302) and *bem1-m1* (YACB303) cells were performed as described (Segall, 1993). Yeast actin was visualized with rhodamine–phalloidin (Molecular Probes, Leiden, The Netherlands) as described previously (Brown *et al*., 1997). The budding pattern was determined by calcofluor white staining (Fluorescent Brightener; Sigma), and quantified by counting at least 200 cells with three or more bud scars (Guthrie and Fink, 1991). GFP-tagged proteins were visualized with a Chroma GFPII filter (excitation 440–470 nm). Photographs were taken on a Zeiss Axiophot fluorescence microscope using a 63× oil objective and recorded with a Photometrics CCD camera. Images were analyzed with Photoshop 4.0 software (Adobe).

Cell cycle synchronization and experiments with Lat-A

G_0–G_1 release experiments in the presence or absence of Latrunculin-A (Lat-A), and G_1 arrest of *cln1*, *2*, *3Δ pMETCLN2* (YMG258) were carried out as described earlier (Jaquenoud and Peter, 2000). The localization of the GFP-tagged proteins was analyzed by fluorescence microscopy. For quantitation, at least 200 cells were counted at each time point.

Supplementary data

Supplementary data for this paper are available at *The EMBO Journal* Online.

Acknowledgements

We thank M.-P.Gulli, J.Heitmann, A.Bender, C.Boone, D.Kellogg, G.Ammerer and D.Lew for providing plasmids, strains and antibodies, and Miranda Sanders and Phil Crews (UCSC) for the synthesis of Latrunculin-A. We are grateful to P.Philipsen for sharing the genome sequence data from *A.gossipii*, P.Wiget for time-lapse microscopy, members of the group for stimulating discussion, and M.-P.Gulli and R.Iggo for critical reading of the manuscript. M.P. and C.Z. are supported by the Swiss National Science Foundation, and M.P. by the Swiss Cancer League and a Helmut Horten Incentive Award.

References

Arkowitz,R.A. (1999) Responding to attraction: chemotaxis and chemotropism in *Dictyostelium* and yeast. *Trends Cell Biol.*, **9**, 20–27.

Ausubel,F.M., Brent,R., Kingston,R.E., Moore,D.D., Seidman,J.G., Smith,J.A. and Struhl,K. (1991) *Current Protocols in Molecular Biology*. Greene Publishing Associates and Wiley-Interscience, New York, NY.

Ayscough,K.R., Stryker,J., Pokala,N., Sanders,M., Crews,P. and Drubin,D.G. (1997) High rates of actin filament turnover in budding yeast and roles for actin in establishment and maintenance of cell polarity revealed using the actin inhibitor Latrunculin-A. *J. Cell Biol.*, **137**, 399–416.

Bender,A. and Pringle,J.R. (1989) Multicopy suppression of the *CDC24* budding defect in yeast by *CDC42* and three newly identified genes including the ras-related gene *RSR1*. *Proc. Natl Acad. Sci. USA*, **86**, 9976–9980.

Bender,A. and Pringle,J.R. (1991) Use of a screen for synthetic lethal and multicopy suppressee mutants to identify two new genes involved in morphogenesis in *S. cerevisiae*. *Mol. Cell. Biol.*, **11**, 1295–1305.

Bender,L., Lo,H.S., Lee,H., Kokojan,V., Peterson,V. and Bender,A. (1996) Associations among PH and SH3 domain-containing proteins and Rho-type GTPases in yeast. *J. Cell Biol.*, **133**, 879–894.

Bose,I., Irazoqui,J.E., Moskow,J.J., Bardes,E.S., Zyla,T.R. and Lew,D.J. (2001) Assembly of scaffold-mediated complexes containing Cdc42, the exchange factor Cdc24 and the effector Cla4 required for cell cycle regulated phosphorylation of Cdc24. *J. Biol. Chem.*, **276**, 7176–7186.

Brown,J.L., Jaquenoud,M., Gulli,M.P., Chant,J. and Peter,M. (1997) Novel Cdc42-binding proteins Gic1 and Gic2 control cell polarity in yeast. *Genes Dev.*, **11**, 2972–2982.

Bucher,P., Karplus,K., Moeri,N. and Hofmann,K. (1996) A flexible motif search technique based on generalized profiles. *Comput. Chem.*, **20**, 3–23.

Butty,A.C., Pryciak,P.M., Huang,L.S., Herskowitz,I. and Peter,M. (1998) The role of Far1 in linking the heterotrimeric G protein to polarity establishment proteins during yeast mating. *Science*, **282**, 1511–1516.

Chang,E.C., Barr,M., Wang,Y., Jung,V., Xu,H.P. and Wigler,M.H. (1994) Cooperative interaction of *S. pombe* proteins required for mating and morphogenesis. *Cell*, **79**, 131–141.

Chant,J. (1999) Cell polarity in yeast. *Annu. Rev. Cell Dev. Biol.*, **15**, 365–391.

Chenevert,J., Corrado,K., Bender,A., Pringle,J. and Herskowitz,I. (1992) A yeast gene (BEM1) necessary for cell polarization whose product contains two SH3 domains. *Nature*, **356**, 77–79.

Drubin,D.G. (2000) *Cell Polarity*. Oxford University Press, Oxford, UK, pp. 1–320.

Gimeno,C.J., Ljungdahl,P.O., Styles,C.A. and Fink,G.R. (1992) Unipolar cell divisions in the yeast *S. cerevisiae* lead to filamentous growth: regulation by starvation and *RAS*. *Cell*, **68**, 1077–1090.

Gulli,M.P. and Peter,M. (2001) Temporal and spatial regulation of Rho-type guanine-nucleotide exchange factors: the yeast perspective. *Genes Dev.*, **15**, 365–379.

Gulli,M.P., Jaquenoud,M., Shimada,Y., Niederhauser,G., Wiget,P. and Peter,M. (2000) Phosphorylation of the Cdc42 exchange factor Cdc24 by the PAK-like kinase Cla4 may regulate polarized growth in yeast. *Mol. Cell*, **6**, 1155–1167.

Guthrie,C. and Fink,G.R. (1991) *Guide to Yeast Genetics and Molecular Biology*. Academic Press, San Diego, CA, 933 pp.

Gyuris,J., Golemis,E., Chertkov,H. and Brent,R. (1993) Cdi1, a human G_1 and S phase protein phosphatase that associates with Cdk2. *Cell*, **75**, 791–803.

Hall,A. (1998) Rho GTPases and the actin cytoskeleton. *Science*, **279**, 509–514.

Harlow,E. and Lane,D. (1988) *Antibodies: A Laboratory Manual*. Cold Spring Harbor Laboratory Press, Cold Spring Harbor, NY.

Ito,T., Matsui,Y., Ago,T., Ota,K. and Sumimoto,H. (2001) Novel modular domain PB1 recognizes PC motif to mediate functional protein–protein interactions. *EMBO J.*, **20**, 3938–3946.

Jaquenoud,M. and Peter,M. (2000) Gic2 may link activated Cdc42 to components involved in actin polarization, including Bni1 and Bud6 (Aip3). *Mol. Cell. Biol.*, **20**, 6244–6258.

Jaquenoud,M., Gulli,M.-P., Peter,L. and Peter,M. (1998) The Cdc42p effector Gic2p is targeted for ubiquitin-dependent degradation by the SCF^{Grr1} complex. *EMBO J.*, **17**, 5360–5373.

Johnson,D.I. (1999) Cdc42: an essential Rho-type GTPase controlling eukaryotic cell polarity. *Microbiol. Mol. Biol. Rev.*, **63**, 54–105.

Kron,S.J. and Gow,N.A. (1995) Budding yeast morphogenesis: signalling, cytoskeleton and cell cycle. *Curr. Opin. Cell Biol.*, **7**, 845–855.

Kron,S.J., Styles,C.A. and Fink,G.R. (1994) Symmetric cell division in pseudohyphae of the yeast *S cerevisiae*. *Mol. Biol. Cell*, **5**, 1003–1022.

Leeuw,T., Fourest,L.A., Wu,C., Chenevert,J., Clark,K., Whiteway,M., Thomas,D.Y. and Leberer,E. (1995) Pheromone response in yeast: association of Bem1 with proteins of the MAP kinase cascade and actin. *Science*, **270**, 1210–1213.

Lengeler,K.B., Davidson,R.C., D'Souza,C., Harashima,T., Shen,W.C., Wang,P., Pan,X., Waugh,M. and Heitman,J. (2000) Signal transduction cascades regulating fungal development and virulence. *Microbiol. Mol. Biol. Rev.*, **64**, 746–785.

Lew,D.J. and Reed,S.I. (1993) Morphogenesis in the yeast cell cycle: regulation by Cdc28 and cyclins. *J. Cell Biol.*, **120**, 1305–1320.

Lew,D.J. and Reed,S.I. (1995) A cell cycle checkpoint monitors cell morphogenesis in budding yeast. *J. Cell Biol.*, **129**, 739–749.

Lyons,D.M., Mahanty,S.K., Choi,K.Y., Manandhar,M. and Elion,E.A. (1996) The SH3-domain protein Bem1 coordinates mitogen-activated protein kinase cascade activation with cell cycle control in *S. cerevisiae*. *Mol. Cell. Biol.*, **16**, 4095–4106.

Nern,A. and Arkowitz,R.A. (1999) A Cdc24–Far1–Gβγ protein complex required for yeast orientation during mating. *J. Cell Biol.*, **144**, 1187–1202.

Park,H.O., Bi,E., Pringle,J.R. and Herskowitz,I. (1997) Two active states of the Ras-related Bud1/Rsr1 protein bind to different effectors to determine yeast cell polarity. *Proc. Natl Acad. Sci. USA*, **94**, 4463–4468.

Peterson,J., Zheng,Y., Bender,L., Myers,A., Cerione,R. and Bender,A. (1994) Interactions between the bud emergence proteins Bem1 and Bem2 and Rho-type GTPases in yeast. *J. Cell Biol.*, **127**, 1395–1406.

Ponting,C.P. (1996) Novel domains in NADPH oxidase subunits, sorting nexins and PtdIns 3-kinases: binding partners of SH3 domains? *Protein Sci.*, **5**, 2353–2357.

Pruyne,D. and Bretscher,A. (2000) Polarization of cell growth in yeast. *J. Cell Sci.*, **113**, 571–585.

Segall,J.E. (1993) Polarization of yeast cells in spatial gradients of α mating factor. *Proc. Natl Acad. Sci. USA*, **90**, 8332–8336.

Terasawa,H., Noda,Y., Ito,T., Hatanaka,H., Ichikawa,S., Ogura,K., Sumimoto,H. and Inagaki,F. (2001) Structure and ligand recognition of the PB1 domain: a novel protein module binding to the PC motif. *EMBO J.*, **20**, 3947–3956.

Tjandra,H., Compton,J. and Kellogg,D. (1998) Control of mitotic events by the Cdc42 GTPase, the Clb2 cyclin and a member of the PAK kinase family. *Curr. Biol.*, **8**, 991–1000.

Valtz,N. and Peter,M. (1997) Functional analysis of *FAR1* in yeast. *Methods Enzymol.*, **283**, 350–365.

Weimbs,T., Low,S.H., Chapin,S., Mostov,K.E., Bucher,P. and Hofmann,K. (1997) A conserved domain is present in different families of vesicular fusion proteins: a new superfamily. *Proc. Natl Acad. Sci. USA*, **94**, 3046–3051.

Received October 22, 2001; revised February 6, 2002; accepted February 13, 2002